Magnetization plateau and quantum phase transition of the $S = ½$ trimerized XXZ spin chain

1999 J. Phys. A: Math. Gen. 32 4601

(http://iopscience.iop.org/0305-4470/32/25/304)

J. Phys. A: Math. Gen. **32** (1999) 4601–4609. Printed in the UK PII: S0305-4470(99)97449-8

Magnetization plateau and quantum phase transition of the $S = \frac{1}{2}$ trimerized XXZ spin chain

Kiyomi Okamoto† and Atsuhiro Kitazawa‡

† Department of Physics, Tokyo Institute of Technology, Oh-Okayama, Meguro-ku, Tokyo 152-8551, Japan

‡ Department of Physics, Kyushu University 33, Fukuoka, 812-8581, Japan

Received 9 September 1998, in final form 25 March 1999

Abstract. We study the plateau of the magnetization curve at $M = M_s/3$ (M_s is the saturation magnetization) of the $S = \frac{1}{2}$ trimerized XXZ spin chain. By examining the level crossing of low-lying excitations obtained from the numerical diagonalization, we precisely determine the phase boundary between the plateau state and the no-plateau state on the $\Delta - t$ plane, where Δ denotes the XXZ anisotropy and t the magnitude of the trimerization. This quantum phase transition is of the Berezinskii–Kosterlitz–Thouless type.

1. Introduction

In recent years the quantized plateau of the magnetization curve of spin chains has attracted much attention. Hida [1] numerically studied the $S = \frac{1}{2}$ ferromagnetic–ferromagnetic–antiferromagnetic trimerized Heisenberg chain and found the plateau of the magnetization curve at $M = M_s/3$ (M_s is the saturation magnetization) for some parameter region of J_F/J_{AF}, where J_F and J_{AF} are the ferromagnetic and antiferromagnetic couplings, respectively. KO [2] analytically investigated Hida's model to clarify the mechanism for the appearance and disappearance of the $M = M_s/3$ plateau. Later related numerical and theoretical findings [3–8, 11, 12, 14] are reported in the literature. The magnetization plateaus are also found experimentally in $S = 1$ Ni compound $[Ni_2(Medpt)_2(\mu\text{-ox})(\mu\text{-}N_3)]ClO_4 \times 0.5H_2O$ [9] and in $S = \frac{1}{2}$ Cu compound NH_4CuCl_3 [10]. The behaviour of the magnetization curve of NH_4CuCl_3 is quite remarkable because magnetization plateaus are observed at $M = (\frac{3}{4})M_s$ and $M = (\frac{1}{4})M_s$ but not at $M = 0$ and $M = (\frac{1}{2})M_s$.

Oshikawa, *et al* [7] gave the necessary condition for the appearance of the magnetization plateau:

$$n(S - \langle m \rangle) = \text{integer} \tag{1}$$

where n is the periodicity of the state, S the magnitude of spins and $\langle m \rangle$ the average magnetization per one spin. Since (1) is the necessary condition, it depends on the details of the models whether the magnetization plateau exists or not, even if condition (1) is satisfied.

In this paper we study the $M = M_s/3$ plateau of the $S = \frac{1}{2}$ trimerized XXZ spin chain described by

$$H = \sum_{j=1}^{L} \{J'[h_{3j-2,3j-1}(\Delta) + h_{3j-1,3j}(\Delta)] + J h_{3j,3j+1}(\Delta)\} \tag{2}$$

0305-4470/99/254601+09$19.50

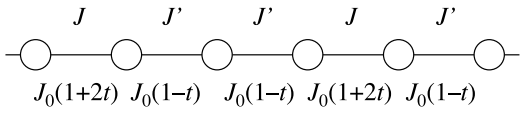

Figure 1. Sketch of the trimerized XXZ chain. The expression of the lower line corresponds to the parametrized form (4).

where

$$h_{lm}(\Delta) = h^{\perp}_{lm} + \Delta h^{z}_{lm} \qquad h^{\perp}_{lm} = S^{x}_{l}S^{x}_{m} + S^{y}_{l}S^{y}_{m} \qquad h^{z}_{lm} = S^{z}_{l}S^{z}_{m}. \tag{3}$$

Our model is sketched in figure 1. Unfortunately there seems to be no report of finding the $M_s/3$ plateau in existing one-dimensional materials to which the present model is applied. However, our model is closely related to a ferromagnetic–ferromagnetic–antiferromagnetic chain $3CuCl_2 \cdot 2$dioxane [1, 13], as will be discussed in section 4.

In section 2 we qualitatively discuss the properties of the transition between the plateau and no-plateau states by use of the bosonized Hamiltonian. In section 3 we determine the phase boundary between the plateau and no-plateau states from the numerical diagonalization data by examining the crossings of the low-lying excitations [15]. Section 4 is devoted to a discussion.

2. Transition between the plateau state and the no-plateau state

It is convenient to parametrize the Hamiltonian (2) as

$$H = J_0 \sum_{j=1}^{L} \{(1-t)[h_{3j-2,3j-1}(\Delta) + h_{3j-1,3j}(\Delta)] + (1+2t)h_{3j,3j+1}(\Delta)\} \tag{4}$$

where

$$J_0 = \frac{2J' + J}{3} \qquad t = -\frac{J' - J}{2J' + J}. \tag{5}$$

The model is sketched in figure 1. The bosonized expression of the Hamiltonian (4) can be obtained by the following procedure:

(a) Transforming (4) into the spinless fermion expression by use of the Jordan–Wigner transformation. The spacing between the neighbouring spins is taken as the unit length.
(b) Linearizing the dispersion relation of the spinless fermions $\omega(k) = J_0 \cos k$ around $k = \pm k_F$, where $k_F \equiv \pi/3$ corresponds to the band filling of $M = M_s/3$. The Fermi velocity at $k = k_F$ is $v_F = (\sqrt{3}/2)J_0$.
(c) Taking the effects of trimerization and the interactions between fermions into account through a procedure similar to that of the standard bosonization technic.

From the above procedure, we obtain the following sine–Gordon Hamiltonian:

$$H = \frac{1}{2\pi}\int \mathrm{d}x \left[v_s K (\pi \Pi)^2 + \frac{v_s}{K}\left(\frac{\partial \phi}{\partial x}\right)^2 \right] + \frac{y_\phi v_s}{2\pi}\int \mathrm{d}x \, \cos\sqrt{2}\phi \tag{6}$$

where v_s is the spin wave velocity of the system, Π is the momentum density conjugate to ϕ, $[\phi(x), \Pi(x')] = \mathrm{i}\delta(x - x')$, and the coefficients v_s, K, and y_ϕ are related to J_0, t and Δ as

$$v_s = \sqrt{3}J_0\sqrt{AC} \qquad K = \frac{1}{2\pi}\sqrt{\frac{C}{A}} \qquad y_\phi v_s = \pi J_0 t(2 + \Delta) \tag{7}$$

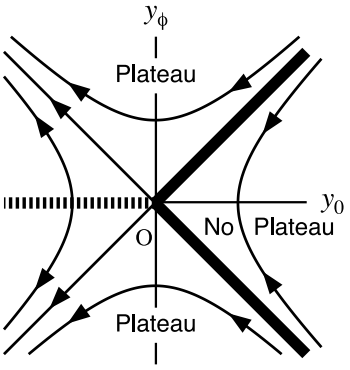

Figure 2. Flow diagram of the renormalization group equation (11). The thick solid lines show the BKT lines and the thick dotted line the Gaussian line.

where

$$A = \frac{1}{8\pi}\left(1 + \frac{5}{\sqrt{3}\pi}\Delta\right) \qquad C = 2\pi\left(1 - \frac{1}{\sqrt{3}\pi}\Delta\right). \tag{8}$$

We note that the expressions for A and C are in the lowest order of Δ. The dual field θ is defined by $\partial_x\theta = \pi\Pi$, and we make the identification $\phi = \phi + \sqrt{2}\pi$, $\theta = \theta + \sqrt{2}\pi$. We note that the umklapp term (which exists in the $M = 0$ case and is important to describe the transition between the spin-fluid state and the Néel state) does not exist, because $2k_F$ is not equal to the reciprocal lattice wavenumbers. The field ϕ is related to the fast varying (in space) part of the spin density $S^z(x)$ in the continuum picture as

$$S^z_{\text{fast}}(x) = \frac{1}{3}\left\{\cos\left(2k_F x - \frac{\pi}{3} + \sqrt{2}\phi\right) + \frac{1}{2}\right\} \tag{9}$$

which makes the physical meaning of ϕ clear. We note that the slowly varying part of the spin density is proportional to $\partial\phi/\partial x$.

As is well known, the excitation spectrum of the sine–Gordon model is either massive or massless depending on the values of K and y_ϕ. In the massive case the $M_s/3$ magnetization plateau exists, and in the massless case it does not [2]. It is convenient to discuss the properties of (6) in the framework of the renormalization group method. The renormalization group equations for (6) are

$$\frac{\mathrm{d}K\,(L)^{-1}}{\mathrm{d}\,\ln L} = \frac{1}{8}y_\phi(L)^2 \qquad \frac{\mathrm{d}y_\phi\,(L)}{\mathrm{d}\,\ln L} = \left(2 - \frac{K(L)}{2}\right)y_\phi(L) \tag{10}$$

where L is an infrared cutoff. Denoting $K(L) = 4(1 + y_0(L)/2)$ near $K(L) = 4$, we obtain

$$\frac{\mathrm{d}y_0\,(L)}{\mathrm{d}\,\ln L} = -y_\phi(L)^2 \qquad \frac{\mathrm{d}y_\phi\,(L)}{\mathrm{d}\,\ln L} = -y_0(L)y_\phi(L) \tag{11}$$

and show its flow diagram in figure 2. The Berezinskii–Kosterlitz–Thouless (BKT) transition occurs at $y_0 = |y_\phi|$, shown by thick solid lines. The BKT nature of the transition between the plateau state and the no-plateau state was first pointed out by one of the present authors (KO) in [2]. At the BKT transition point, by substituting $y_0 = |y_\phi|$ into equation (11), we have

$$y_0(L) = \frac{y_0}{y_0\ln(L/L_0) + 1} \tag{12}$$

where y_0 is the bare value. When $y_0 < 0$ (i.e., $K < 4$), any small (but not equal to zero) amount of trimerization brings about the magnetization plateau. The phase boundary between two plateau regions is a Gaussian line (thick dotted line), on which the critical exponents varies

continuously. In the no-plateau region, the effect of the trimerization vanishes in the sense of the renormalization group due to the strong quantum fluctuations.

We note that it is dangerous to apply the conventional phenomenological renormalization group method to the BKT transition, as is fully discussed in [16].

3. Numerical approach

The scaling dimension of the primary field $\mathcal{O}_{m,n} = \exp(m\sqrt{2}\phi + n\sqrt{2}\theta)$ for $y_\phi = 0$ is given by

$$x_{n,m} = \frac{K}{2}m^2 + \frac{1}{2K}n^2 \tag{13}$$

where n and m are integers with the periodic boundary condition (PBC). According to the finite-size scaling theory by Cardy [17, 18], the excitation energy of the finite-size system at a critical point is related to the scaling dimension as

$$x_{m,n}(L) = \frac{L}{2\pi v_s}(E_{m,n}(L) - E_g(L)) \tag{14}$$

where $E_g(L)$ is the ground state energy of the L-spin system with PBC. Near the BKT transition ($K \approx 4$), the excitation energy is written as

$$\frac{L}{2\pi v_s}\Delta E_{m,0}(L) = 2m^2 + y_0(L)m^2 \tag{15}$$

$$\frac{L}{2\pi v_s}\Delta E_{0,n}(L) = \frac{1}{8}n^2 - y_0(L)\frac{1}{16}n^2 \tag{16}$$

for integer m, n. Thus, considering equation (12), we have the logarithmic corrections for a finite-size spectrum.

To determine the BKT transition point, we use the method developed by Nomura and Kitazawa [15], in which the level crossings for some excitations are used. With the twisted boundary condition (TBC) $S^{x,y}_{3L+1} = -S^{x,y}_1$, $S^z_{3L+1} = S^z_1$, the integer m in the operator $\mathcal{O}_{m,n}$ shifts to $m+\frac{1}{2}$ as $\mathcal{O}_{m,n} \to \mathcal{O}_{m+1/2,n}$. For the scaling dimensions of the operators $\sqrt{2}\cos(\phi/\sqrt{2})$ and $\sqrt{2}\sin(\phi/\sqrt{2})$ we have the following finite-size corrections:

$$\begin{aligned} x^{\mathrm{c}}_{1/2,0}(L) &= \tfrac{1}{2} + \tfrac{1}{4}y_0(L) + \tfrac{1}{2}y_\phi(L) \\ x^{\mathrm{s}}_{1/2,0}(L) &= \tfrac{1}{2} + \tfrac{1}{4}y_0(L) - \tfrac{1}{2}y_\phi(L). \end{aligned} \tag{17}$$

Note that scaling dimensions $x^{\mathrm{c,s}}_{1/2,0}$ are not of the form of (15). This comes from the first-order perturbation of the second term ($\cos\sqrt{2}\phi$ term) in equation (6). Denoting $y_\phi = \pm y_0(1+w)$ where w measures the distance from the BKT transition point, we have for $y_\phi > 0$

$$\begin{aligned} x^{\mathrm{c}}_{1/2,0}(L) &= \tfrac{1}{2} + \tfrac{3}{4}y_0(L)(1 + \tfrac{2}{3}w) \\ x^{\mathrm{s}}_{1/2,0}(L) &= \tfrac{1}{2} - \tfrac{1}{4}y_0(L)(1 + 2w) \end{aligned} \tag{18}$$

and for $y_\phi < 0$

$$\begin{aligned} x^{\mathrm{c}}_{1/2,0}(L) &= \tfrac{1}{2} - \tfrac{1}{4}y_0(L)(1 + 2w) \\ x^{\mathrm{s}}_{1/2,0}(L) &= \tfrac{1}{2} + \tfrac{3}{4}y_0(L)(1 + \tfrac{2}{3}w). \end{aligned} \tag{19}$$

On the other hand, from equation (16) the scaling dimension of $\mathcal{O}_{0,\pm 2}$ is given by

$$x_{0,\pm 2}(L) = \tfrac{1}{2} - \tfrac{1}{4}y_0(L) \tag{20}$$

from which we see that $x_{0,\pm 2}$ and $x^{\mathrm{c,s}}_{1/2,0}$ (s for $y_\phi > 0$ and c for $y_\phi < 0$) cross linearly at the BKT transition point ($w = 0$).

In order to identify the excitations with those of the sine–Gordon model (6), we can use the following symmetry. The Hamiltonian with PBC is invariant under the spin rotation around the z axis, the translation by three sites, ($\boldsymbol{S}_j \to \boldsymbol{S}_{j+3}$), and space inversion ($\boldsymbol{S}_j \to \boldsymbol{S}_{L-j+1}$). Corresponding eigenvalues are M, the wavenumber q, and $P = \pm 1$. The space inversions in the sine–Gordon model are

$$\phi \to -\phi \qquad \theta \to \theta + \pi/\sqrt{2} \qquad x \to -x. \tag{21}$$

The magnetization M is related to n as $n = M_s/3 - M$. The 'ground state' energy E_g is the lowest one with $[M = M_s/3, q = 0, P = 1]$.

In our model, the energy level corresponding to the operator $\mathcal{O}_{0,\pm 2}$ is $E_0(M_s/3 \pm 2, 0, 1)$, where $E_0(M, q, P)$ is the lowest energy with $[M, q, P]$. However, we cannot directly compare the energies with different M. In the language of the spinless fermions, the difference in M corresponds to the difference in the number of fermions, N. Thus to compare the energies with different M, we should use $E - \mu N$, where μ is the chemical potential of the spinless fermions. Since μ near $M_s/3$ is expressed as

$$\mu = \frac{1}{4}\left\{E_0\left(\frac{M_s}{3} + 2, 0, 1\right) - E_0\left(\frac{M_s}{3} - 2, 0, 1\right)\right\} \tag{22}$$

the excitation energy corresponding to $\mathcal{O}_{0,2}$ is

$$\begin{aligned}\Delta E_{0,2} &= \left\{E_0\left(\frac{M_s}{3} + 2, 0, 1\right) - E_0\left(\frac{M_s}{3}, 0, 1\right) - 2\mu\right\} \\ &= \frac{1}{2}\left\{E_0\left(\frac{M_s}{3} + 2, 0, 1\right) + E_0\left(\frac{M_s}{3} - 2, 0, 1\right)\right\} - E_0\left(\frac{M_s}{3}, 0, 1\right).\end{aligned} \tag{23}$$

The same expression is obtained for $\mathcal{O}_{0,-2}$. Equation (23) can also be obtained by use of the Legendre transformation $E \to E - HM$.

The excitation energies corresponding to the operators $\sqrt{2}\cos(\phi/\sqrt{2})$ and $\sqrt{2}\sin(\phi/\sqrt{2})$ are obtained by the two lowest energies $\Delta E(M, P)$ with the twisted boundary condition as

$$\begin{aligned}\Delta E^{c}_{1/2,0} &= E^{\mathrm{TBC}}\left(\frac{M_s}{3}, 1\right) - E\left(\frac{M_s}{3}, 0, 1\right) \\ \Delta E^{s}_{1/2,0} &= E^{\mathrm{TBC}}\left(\frac{M_s}{3}, -1\right) - E\left(\frac{M_s}{3}, 0, 1\right)\end{aligned} \tag{24}$$

where $E(M_s, 0, 1)$ is the lowest energy with PBC. The excitation energies $\Delta E_{0,\pm 2}$ and $\Delta E^{c,s}_{1/2,0}$ (s for $y_\phi > 0$ and c for $y_\phi < 0$) should cross linearly at the BKT transition point.

Figure 3 shows the behaviour of $\Delta E_{0,\pm 2}$ and $\Delta E^{c}_{1/2,0}$ for $L = 18$ spins as functions of anisotropy parameter Δ when $t = -0.25$. From the crossing point, we obtain $\Delta_c = -0.8389$ for $L = 18$ spins. The BKT transition point for the infinite system can be obtained by extrapolating the Δ_c data to $L = \infty$, as shown in figure 4. Thus, we can draw the phase diagram figure 5 on the $\Delta - t$ plane. The point M ($\Delta = -0.729$) is the multicritical point where two BKT lines meet together into the Gaussian line (shown by the thick dotted line) on which the critical exponents vary continuously. The $\Delta \leqslant -1$ region is the ferromagnetic region.

In order to check the consistency, let us confirm the conformal anomaly $c = 1$ which is related to the leading finite-size correction of the 'ground state' energy with PBC as [19, 20]

$$E_g(L) = L\epsilon_g - \frac{\pi v_s c}{6L} + \cdots \tag{25}$$

where ϵ_g the energy per one spin for the infinite-size system. The spin wave velocity v_s can be obtained by

$$v_s = \lim_{L\to\infty} \frac{L\Delta E(q = 2\pi/L)}{2\pi} \tag{26}$$

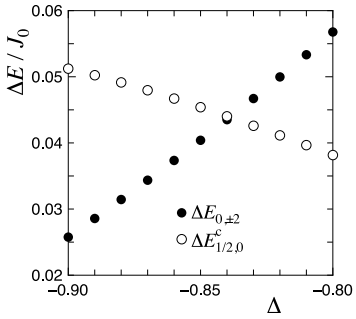

Figure 3. $\Delta E_{0,\pm 2}$ and $\Delta E^{c}_{1/2,0}$ for $L = 18$ spins as functions of anisotropy parameter Δ when $t = -0.25$. From the crossing point we obtain $\Delta_c(L = 18) = -0.8389$.

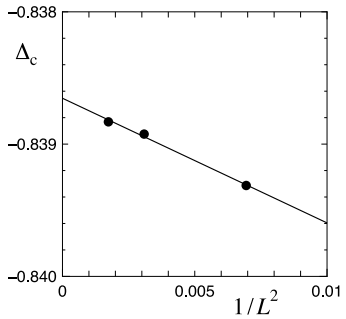

Figure 4. Extrapolation of Δ_c to $L = \infty$ when $t = -0.25$. We obtain $\Delta_c = -0.839$.

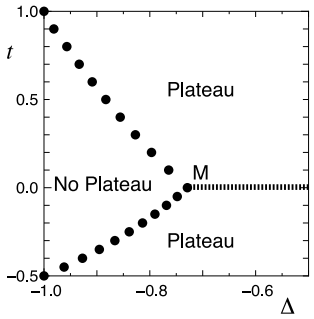

Figure 5. Phase diagram on the $\Delta - t$ plane. Closed circles are the BKT transition point determined from the numerical data as explained in the text. The thick dotted line denotes the Gaussian line. The multicritical point M corresponds to the point O of figure 2.

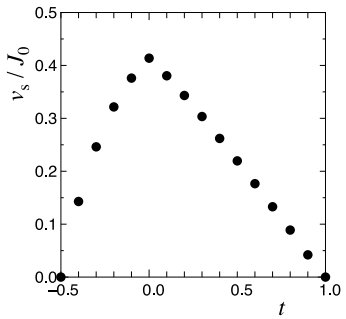

Figure 6. Spin wave velocity on the BKT transition line.

where $\Delta E(q = 2\pi/L)$ is the lowest excitation energy having the wavenumber $q = 2\pi/L$ in the $M = M_s/3$ space. Thus we can check the value of c by use of equations (25) and (26). We have found that $c = 1$ is realized on the BKT line within the error of a few per cent. For instance, in the case of $(t, \Delta) = (0.5, -0.881)$ on the BKT line, we obtain $v_s c = 0.212 J_0$ through equation (25) and $v_s = 0.217 J_0$ through equation (26). Figure 6 shows the spin wave velocity v_s on the BKT transition line.

From equations (17) and (20), we can eliminate the leading logarithmic correction at the transition point ($w = 0$) using the following average:

$$\begin{aligned} \frac{3x^{s}_{1/2,0}(L) + x^{c}_{1/2,0}(L)}{4} &= \frac{1}{2} \qquad \text{for} \quad y_\phi > 0 \\ \frac{3x^{c}_{1/2,0}(L) + x^{s}_{1/2,0}(L)}{4} &= \frac{1}{2} \qquad \text{for} \quad y_\phi < 0. \end{aligned} \tag{27}$$

This relation is appropriate to the consistency check. The averaged scaling dimension equation (27) on the BKT line is shown in figure 7. We can see that the averaged scaling dimension is very close to $\frac{1}{2}$, which guarantees the consistency of our numerical method.

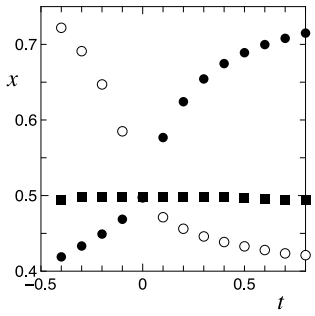

Figure 7. Scaling dimension on the BKT line. Closed circles are $x^{\mathrm{c}}_{1/2,0}(L)$, open circles $x^{\mathrm{s}}_{1/2,0}(L)$ and closed squares the averaged scaling dimension (27).

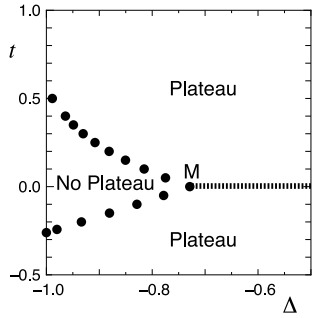

Figure 8. Phase diagram of the 'xy-trimerization model'.

4. Discussion

We have obtained the phase diagram on the $\Delta - t$ plane as shown in figure 5. Two BKT lines meet together into the Gaussian line at the multicritical point M where $\Delta = \Delta_{\mathrm{M}} = -0.729$. If we put $K = 4$ in equations (7) and (8), we obtain $\Delta_{\mathrm{M}} = -3\sqrt{3}\pi/21 = -0.777$. This value is slightly different from $\Delta_{\mathrm{M}} = -0.729$, because the expression (8) is valid in the lowest order of Δ near $\Delta = 0$. In the absence of the trimerization ($t = 0$), the present model is reduced to the usual $S = \frac{1}{2}$ XXZ chain, which is solvable by the Bethe ansatz. The numerical solution of the Bethe ansatz equations leads to $\Delta_{\mathrm{M}} = -0.729\,043$ for $M = M_{\mathrm{s}}/3$ and $K = 4$ [12, 21, 22], which just agrees with our numerical values.

In figure 5, the slopes of the BKT lines for $t > 0$ and $t < 0$ near the multicritical point M are the same as each other. This can be explained from the symmetry of the bosonized Hamiltonian (6). Hamiltonian (6) is invariant under the transformation $t \leftrightarrow -t$ and $\sqrt{2}\phi \leftrightarrow \sqrt{2}\phi + \pi$. Away from the multicritical point M, on the other hand, the BKT lines on the upper and lower planes are asymmetric with each other, as can be seen from figure 5. This is quite reasonable because the $t \leftrightarrow -t$ symmetry does not hold in the original spin Hamiltonian (4). From the standpoint of the bosonized Hamiltonian, this comes from the existence of higher-order terms [23] $\cos(2\sqrt{2}\phi)$, $\cos(4\sqrt{2}\phi)$, ..., of which coefficients are also proportional to the trimerization parameter t. If these higher-order terms are taken into account, the symmetry of the bosonized Hamiltonian under the transformation $t \leftrightarrow -t$ and $\sqrt{2}\phi \leftrightarrow \sqrt{2}\phi + \pi$ is lost, which explains the asymmetry of the BKT lines.

The mass-generating term in (6) is

$$\frac{J_0 t\,(2 + \Delta)}{2} \int \mathrm{d}x\ \cos(\sqrt{2}\phi). \tag{28}$$

In the factor $2 + \Delta$, the first term comes from the x and y components of the trimerization, and the second term from the z component. When $\Delta < 0$, they are competing. In the $S = \frac{1}{2}$ ferromagnetic–antiferromagnetic alternating chain [24, 25], this kind of competition brings about the transition between the Haldane state and the large-D state. In our case, however, this competition only reduces the effect of the trimerization. In fact, we obtain the phase diagram figure 8 for the 'xy-trimerization model' in which the trimerization exists only in the $J^x - J^x$ and $J^y - J^y$ couplings and not in the $J^z - J^z$ coupling. We see that the trimerization effect is reduced in figure 5 in comparison to figure 8, because the no-plateau region is wider in figure 5 than in figure 8. We note that the phase boundary of the ferromagnetic region is no longer $\Delta = -1$, because the $SU(2)$ symmetry is broken even at $\Delta = -1$ in the xy-trimerization

model. This situation is similar to the $S = \frac{1}{2}$ XXZ chain under the staggered magnetic field [26]. This phase boundary can be calculated from the instability of the ferromagnetic state against the $M = M_s - 1$ spin wave excitation, resulting in

$$\Delta = -\frac{1 + 2t + \sqrt{9 - 12t + 12t^2}}{4}. \tag{29}$$

The present model is closely related to the ferromagnetic–ferromagnetic–antiferromagnetic chain [1] described by

$$H_{\mathrm{FFA}} = \sum_{j=1}^{L} \{-J_{\mathrm{F}}(\boldsymbol{S}_{3j-2} \cdot \boldsymbol{S}_{3j-1} + \boldsymbol{S}_{3j-1} \cdot \boldsymbol{S}_{3j}) + J_{\mathrm{A}} \boldsymbol{S}_{3j} \cdot \boldsymbol{S}_{3j+1}\} \tag{30}$$

where $J_{\mathrm{F}} > 0$ is the ferromagnetic coupling and J_{A} the antiferromagnetic coupling. We note that $3CuCl_2 \cdot 2$dioxane is well modelled by H_{FFA} [13]. This model can be transformed into [2]

$$\begin{aligned} \tilde{H} = {} & J_0(1 - 2t_\perp) \sum_j h^{\perp}_{3j-1,3j} + J_0(1 + t_\perp) \sum_j (h^{\perp}_{3j,3j+1} + h^{\perp}_{3j+1,3j+2}) \\ & + J_0(\Delta_0 - 2t_z) \sum_j h^{z}_{3j-1,3j} + J_0(\Delta_0 + t_z) \sum_j (h^{z}_{3j,3j+1} + h^{z}_{3j+1,3j+2}) \end{aligned} \tag{31}$$

where

$$\begin{aligned} J_0 &= \frac{2J_{\mathrm{F}} + J_{\mathrm{A}}}{3} \qquad \Delta_0 = \frac{-2\gamma + 1}{2\gamma + 1}\Delta \\ t_\perp &= \frac{\gamma - 1}{2\gamma + 1} \qquad t_z = -\frac{\gamma + 1}{2\gamma + 1}\Delta \qquad \gamma = \frac{J_{\mathrm{F}}}{J_{\mathrm{A}}} \end{aligned} \tag{32}$$

which is a generalized version of our model (2) if parameters Δ_0, $t_\perp$ and T_z run independently of one another. Thus the same method can be applied to the model (30), to obtain $\gamma_c \simeq 15.4$, where the $M_s/3$ plateau exists for $\gamma < \gamma_c$. Details of the numerical study of the model (30) will be reported elsewhere.

Note added in proof. Very recently, Tanaka's group [27] experimentally studied the magnetic properties of a trimerized $S = \frac{1}{2}$ chain $Cu_3Cl_6(H_2O)_2 \cdot 2H_8C_4SO_2$. We thank K Tanaka for showing us their experimental data prior to publication and for fruitful discussion.

Acknowledgments

We would like to express our appreciation to K Nomura and M Oshikawa for fruitful discussions. We also thank A Honecker for useful comment. A part of the numerical calculation was done using program package TITPACK Ver.2 coded by H Nishimori.

References

[1] Hida K 1994 *J. Phys. Soc. Japan* **63** 2359
[2] Okamoto K 1996 *Solid State Commun.* **98** 245
[3] Roji M and Miyashita S 1996 *J. Phys. Soc. Japan* **65** 1994
[4] Tonegawa T, Nakao T and Kaburagi M 1996 *J. Phys. Soc. Japan* **65** 3317
[5] Tonegawa T, Nishida T and Kaburagi M 1998 *Physica* B **246–7** 368
[6] Totsuka K 1997 *Phys. Rev.* B **57** 3454
[7] Oshikawa M, Yamanaka M and Affleck I 1997 *Phys. Rev. Lett.* **78** 1984
[8] Sakai T and Takahashi M 1998 *Phys. Rev.* B **57** R3201
[9] Narumi Y, Hagiwara M, Sato R, Kindo K, Nakano H and Takahashi M 1998 *Physica* B **246–7** 509

[10] Shiramura W, Takatsu K, Kurniawan B, Tanaka H, Uekusa H, Ohashi Y, Takizawa K, Mitamura H and Goto T 1998 *J. Phys. Soc. Japan* **67** 1548
[11] Cabra D C, Honecker A and Pujol P 1998 *Phys. Rev.* B **58** 6241
[12] Cabra D C and Grynberg M D 1999 *Phys. Rev.* B **59** 119
[13] Ajiro Y, Asano T, Inami T, Aruga-Katori H and Goto T 1994 *J. Phys. Soc. Japan* **63** 859
[14] Honecker A 1999 *Phys. Rev.* B **59** 6790
[15] Nomura K and Kitazawa A 1998 *J. Phys. A: Math. Gen.* **31** 7341
[16] Okamoto K and Nomura K 1996 *J. Phys. A: Math. Gen.* **26** 2279
[17] Cardy J L 1984 *J. Phys. A: Math. Gen.* **17** L385
[18] Cardy J L 1986 *Nucl. Phys.* B **270** 186
[19] Blöte H W J, Cardy J L and Nightingale M P 1986 *Phys. Rev. Lett.* **56** 742
[20] Affleck I 1986 *Phys. Rev. Lett.* **56** 746
[21] Honecker A 1998 Private communication
[22] Honecker webpage http://www.he.sissa.it/˜honecker/roc.html
(webpage http://thew02.physik.uni-bonn.de/˜honecker/roc.html)
[23] Haldane F D M 1981 *Phys. Rev. Lett.* **47** 1840
Haldane F D M 1981 *Phys. Rev. Lett.* **48** 569
[24] Okamoto K, Nishino D and Saika Y 1993 *J. Phys. Soc. Japan* **62** 2587
[25] Okamoto K 1996 *J. Phys. A: Math. Gen.* **29** 1639
[26] Alcaraz F C and Malvetti A L 1995 *J. Phys. A: Math. Gen.* **28** 1521
[27] Tanaka J 1999 Private communication